Analyst



View Journal | View Josue



PAPER

Cite this: Analyst, 2016, 141, 6018

CrossMark

Closed bipolar electrode-enabled dual-cell electrochromic detectors for chemical sensing

Wei Xu, a Kaiyu Fu, a Chaoxiong Ma and Paul W. Bohn*a, b

Bipolar electrodes (BPE) are electrically floating metallic elements placed in electrified fluids that enable the coupling of anodic and cathodic redox reactions at the opposite ends by electron transfer through the electrode. One particularly compelling application allows electron transfer reactions at one end of a closed BPE to be read out optically by inducing a redox-initiated change in the optical response function of a reporter system at the other end. Here, a BPE-enabled method for electrochemical sensing based on the electrochromic response of a methyl viologen (MV) reporter is developed, characterized, and rendered in a field-deployable format. BPE-enabled devices based on two thin-layer-cells of ITO and Pt were fabricated to couple an analytical reaction in one cell with an MV reporter reaction, producing a color change in the complementary cell. Using $Fe(CN)_6^{3/4-}$ as a model analyte, the electrochemically induced color change of MV was determined initially by measuring its absorbance via a CCD camera coupled to a microscope. Then, smartphone-based detection and RGB analysis were employed to further simplify the sensing scheme. Both methods produced a linear relationship between the analyte concentration, the quantity of MV generated, and the colorimetric response, yielding a limit of detection of 1.0 µM. Similar responses were observed in the detection of dopamine and acetaminophen. Further evolution of the device replaced the potentiostat with batteries to control potential, demonstrating the simplicity and portability of the device. Finally, the physical separation of the reporter and analytical cells renders the device competent to detect analytes in different (e.g. non-aqueous) phases, as demonstrated by using the electrochromic behavior of aqueous MV to detect ferrocene in acetonitrile in the analytical cell.

Received 21st June 2016, Accepted 7th September 2016 DOI: 10.1039/c6an01415a

www.rsc.org/analyst

Introduction

Bipolar electrochemistry, which relies on redox reactions occurring at the opposite ends of bipolar electrodes (BPE), provides a new paradigm for electrochemical sensing - one with excellent sensitivity, versatility, and the capability to implement multiplex sensing.^{1,2} BPEs are typically constructed from a non-biased electronic conductor placed in direct contact with a fluid supporting an electric field, i.e., an electrified fluid. The potential gradient in the fluid maps onto the isopotential of the BPE, creating interfacial potential differences between the poles of the BPE and the electrolyte solution in contact with them - oxidizing at one end and reducing at the other. 1,3 Modulation of this potential difference allows two distinct redox reactions to be coupled at the two ends (poles) of the BPE. 1,3,4 By exploiting the compositional and geometric variety available to BPEs, various applications including material preparation and fabrication,5-10 electrochemical

sensing,^{11–13} catalysis screening,^{14–16} micro swimmers,^{17–19} and bipolar electrode focusing^{20–23} have been demonstrated.

Depending on the purpose of the design, BPEs can be operated in either an open or closed configuration. In the open BPE, both cathode and anode are placed in the same fluid, typically inside a microchannel.²⁴⁻²⁶ On the other hand, closed BPE systems involve a single BPE in contact with physically isolated, and possibly chemically distinct, solutions connected to the anodic and cathodic poles of the BPE. 27,28 Since there is no fluid path connecting the anodic and cathodic poles of a closed BPE, the two half redox reactions at the poles of the BPE must be coupled by electron transport through the BPE.²⁷ A major advantage of the closed BPE geometry is the physical isolation of the two redox systems, which simplifies the reaction scheme and eliminates possible interferences in chemical sensing. 1,29 Since the closed BPE setup is analogous to two electrochemical cells in series, remote control or detection can be achieved.²⁸ Accordingly, disposable analytical reaction cells can be coupled to the same reporter, which can be used repeatedly. In addition, because the detection reaction is independent of the analytical reaction, the analytes and the reporter can be in solutions with completely different properties. Similarly, detection is not limited to amperometry.³⁰

^aDepartment of Chemistry and Biochemistry, University of Notre Dame, Notre Dame, IN 46556. USA. E-mail: pbohn@nd.edu

^bDepartment of Chemical and Biomolecular Engineering, University of Notre Dame, Notre Dame, IN 46556, USA

For example, anodic dissolution of a metal film, which can be visually observed, has been used as a simple sensing scheme for BPE electrochemistry. 14-16 More importantly, the closed BPE design can overcome the limitation of electrochemical methods for simultaneously measuring responses at multiple electrodes, such as electrode arrays.26 Indeed, electrochemiluminescence (ECL)^{11,29,31-33} and fluorescence³⁴⁻³⁶ have been coupled to analytical reactions through BPEs, not only improving measurement sensitivity, but also enabling high throughput, parallel sensing. Indirect BPE sensing for biorelevant targets such as 1,4-naphthoquinone and dopamine has been demonstrated based on pH gradients monitored by fluorescence imaging.³⁷ Recently, by coupling fluorescence imaging with electrochemical reactions at bipolar interdigitated electrode arrays, we have shown that it is possible to translate the electron transfer event to a luminescence signal, allowing multiplex detection in a microfluidic system.³⁸ These experiments exhibit the advantage of luminescence readout near zero-background signal - as well as high spatial and temporal resolution.

A drawback of ECL and fluorescence reporting is that they typically require sophisticated equipment and optical alignment for data collection. Colorimetric detection, on the other hand, is based on the color change of an indicator and is a straightforward and inexpensive way to capture the converted analyte signal.39-43 Among various colorimetric indicators, electrochromic materials are interesting, because they involve a shift in the absorption spectrum upon changing the redox state of the molecule. 44,45 This property can be used to report redox events by coupling the electrochemical reactions of an analyte to that of an electrochromic indicator using a closed BPE. Depending on the requirements of the detection scheme, the indicator color change accompanying the analyte redox reaction can be monitored by a spectrometer⁴⁶ or imaging device, 47 such as a charge-coupled device (CCD) or flat-bed scanner, or even by direct visual observation.

In recent years, smartphones have been used as convenient tools for colorimetry, owing to their capability of capturing images with built-in camera and data processing capabilities. 48-52 Smartphone colorimetry opens up new opportunities for simple, fast, and reliable detection, demonstrating potential for point-of-care and real-time diagnosis applications. In order to combine the advantages of BPE with colorimetry for electrochemical sensing, a colorimetric electrochemical sensor was developed using two ITO thin-layer cells to construct isolated analytical and reporter cells connected by a closed BPE. A redox indicator, methyl viologen (MV), which changes from a colorless oxidized state to a dark purple reduced state, was used as the reporter.46 The BPE-enabled electrochemical sensor was evaluated using the MV color change to construct a working curve for Fe(CN)₆^{3/4-}, as initially determined by a CCD camera coupled to an optical microscope. The color response of MV and its dependence on analyte concentration were also measured by smartphone and analyzed by RGB analysis of the resulting color images, demonstrating the capability of the method for monitoring electrochemical reactions at μM analyte concentrations. The same scheme was applied to the detection of dopamine and acetaminophen, confirming the applicability of the methods for different analytes with similar sensitivity. In order to further simplify the detection scheme, AA batteries were employed in place of a potentiostat to drive the electrochemical reaction. The results, which are in reasonable agreement with potentiostat-controlled voltammetry indicate the promise of the BPE-enabled device as a portable electrochromic sensor. Finally, the chemical independence of the analytical and detection regions was demonstrated by using ferrocene in acetonitrile as analyte, while the reaction was readout by monitoring the color change of aqueous MV by both CCD camera and smartphone.

Experimental section

Chemicals and materials

Methyl viologen, dopamine hydrochloride, tetrabutylammonium tetraphenylborate, ferrocene, acetaminophen, and acetonitrile (Sigma-Aldrich), potassium chloride and potassium ferricyanide (Fisher Scientific) and poly(dimethylsiloxane) (PDMS) (Sylgard, 184, Dow Corning) were all used as received. Tape (Scotch) and indium tin oxide (ITO) (70–100 Ω and 8–12 Ω) coated glass slides (Sigma-Aldrich and Delta Technologies) were used for device fabrication. All reagents were analytical grade.

Device assembly and colorimetric measurements

Electrochromic sensor devices were constructed to include analytical and reporter cells, connected by a closed BPE. A glass slide coated by Ti/Pt (Ti 10 nm, Pt 100 nm) was used as a working electrode (WEa) in the analytical cell. The analytical cell (1.5 cm \times 2.5 cm) was fabricated by placing tape (50 μ m thick) around the periphery to act as a spacer between the analytical cell working electrode, WEa, and the ITO BPE. The structure of the reporter cell was similar to that of the analytical cell, except that instead of using a Ti/Pt coated slide, an ITO slide was employed as counter/quasi reference electrode (CE/QRE) (Fig. 1). A small (1 mm \times 1 mm) observation window was opened in the tape spacer and filled with indicator solution, 10 mM methyl viologen in 0.1 M KCl. The BPE was composed of the top ITO electrode in both analytical and reporter cells connected to each other by Cu wire. For the non-aqueous experiments, the tape spacer was replaced by a thin PDMS wall in the in the analytical region because the organic solvent used, i.e. acetonitrile, is incompatible with adhesive tape. Nonaqueous experiments were conducted in acetonitrile with 0.1 M tetrabutylammonium tetraphenylborate, TBATPB, as background electrolyte.

Electrochemical measurements were performed on a commercial potentiostat (CHI 842C, CH Instruments). Potentials ranging from +2.0 V to +3.0 V were applied to WE_a to drive the redox reaction in the analytical cell. Color change of the MV indicator solution was measured on an epifluorescence

Paper Analyst

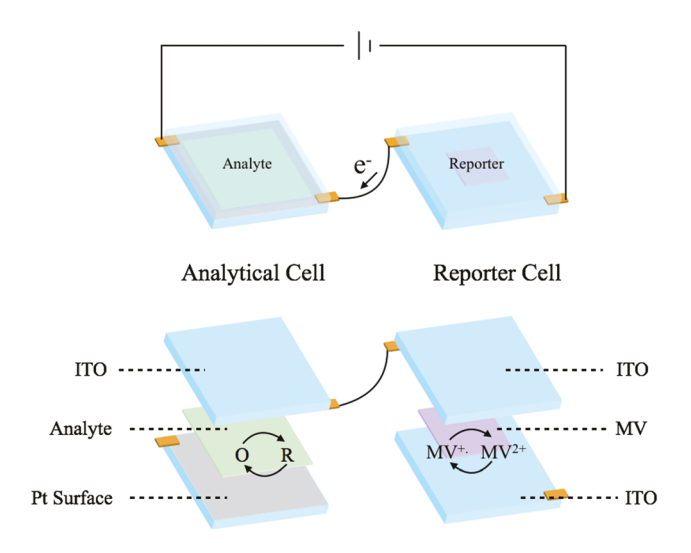


Fig. 1 Schematic illustration of the closed BPE-enabled electrochromic sensor architecture.

microscope (IX-71, Olympus) equipped with appropriate filter set (pass band 510-560 nm) (Chroma Technology Inc.). The intensity data were collected by an electron-multiplier CCD camera (PhotonMax512, Princeton Instruments) at 6 frames per second. In smartphone-based detection, images were acquired with an iPhone 6 (Apple) equipped with a macro lens (Olloclip) at 21× magnification with images acquired 16 mm above the device. The camera was operated in manual mode with parameters set as follows: ISO sensitivity: 100; shutter speed: 1/20 s; white balance: auto. Images were stored in RAWformat, and the red-green-blue readout (RGB) of each image was analyzed by ImageJ software. In experiments employing battery-based potentials, potential was applied by two AA batteries (Energizer) in place of the potentiostat.

Results and discussion

Methyl viologen as an electrochromic reporter

The electrochromic molecule, methyl viologen (MV²⁺), was used as the indicator in the reporter cell of the device. Fig. 2(a) shows the cyclic voltammetry (CV) of MV²⁺ at the ITO working electrode. The waves indicate two successive reversible, oneelectron transfer processes. Negative applied potentials lead to the reduction of colorless MV2+ to a purple MV++ and then, if sufficiently negative, ultimately to the fully reduced MV. In addition, the purple MV*+ can disproportionate into yellow MV and colorless MV²⁺ upon the removal of negative potential. Thus, the color change between colorless and purple is reversible, since the other half reaction occurring at the CE involves the oxidation of MV back to MV2+. To quantify the color change, a CCD camera coupled to an epi-illumination microscope measured the change of absorbance of MV in potential step experiments. As shown in Fig. 2(b), the light absorption increases significantly at -1.0 V, and recovers to the baseline level when the potential is returned to 0 V. The reversibility of

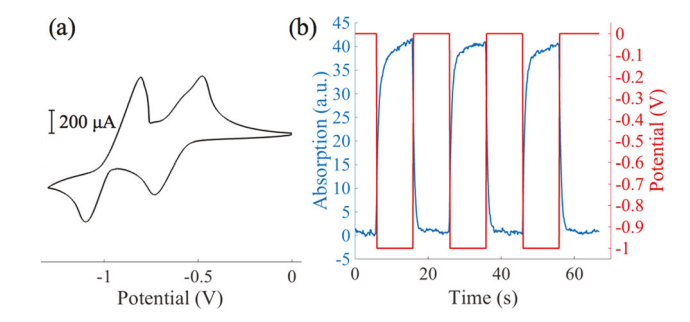


Fig. 2 (a) Cyclic voltammogram of 10 mm methyl viologen in 0.1 m aqueous KCl at a scan rate of 100 mV s⁻¹. (b) Relative absorption of mv in the reporter cell (left) and applied potential (right) as a function of time as measured by a ccd detector on an optical microscope with 20x magnification.

the potential-dependent absorption change indicates that MV can be employed as a reusable electrochromic indicator. In addition, the process of color change, as well as the recovery of the colorless MV²⁺ state, can be easily monitored by CCD or smartphone camera or by direct visual observation.

BPE-enabled colorimetry

The colorimetric reporter cell was filled with MV²⁺ and then coupled to the analytical cell employing a Pt film working electrode (WEa). An ITO electrode was used in the reporter cell, because it has good conductivity and transparency, allowing the BPE-enabled electrochromic color change to be monitored. Fe(CN)₆³⁻ was added to the analytical cell at different concentrations, and positive potential pulses were applied to WEa. In accord with the operating principles of closed BPE structures, reduction of Fe(CN)₆³⁻ to Fe(CN)₆⁴⁻ at the analytical cell end of the BPE, i.e. BPEa, is accompanied by a complementary oxidation of $Fe(CN)_6^{4-}$ to $Fe(CN)_6^{3-}$ at WE_a . Although $Fe(CN)_6^{4-}$ was not added as an initial analyte, the thin-layer-cell geometry, allowing rapid diffusion of the redox product, enables the coupling reactions of Fe(CN)₆^{3/4-} in the analytical cell, which are similar to those redox cycling reactions occurring in a dual electrode system. 53,54 The reduction reaction at BPEa is counterbalanced by the oxidation of purple MV*+ to colorless MV2+ at the reporter cell end of the BPE, i.e. BPE, and the reduction MV²⁺ to MV⁺⁺ at the CE, as confirmed by the reversible color change between colorless and purple in the reporter cell. Similarly, MV*+ was not added to the reporter cell but rather generated by the reduction of MV2+ at the CE, which moves rapidly to the BPE_r. Thus, the efficiency of the closed BPE electrochromic detector scheme depends intimately on the coupling of redox reactions in both cells, which, in turn, depends strongly on fabricating a cell with an optimized gap between BPE_r and CE.

Fig. 3(a) shows the change in light absorption measured by the CCD camera in the reporter cell during application of a potential pulse (5 s at +3.0 V) applied to WEa. A control experiment using 0.1 M KCl without Fe(CN)₆³⁻ exhibited negligible color change in the reporter cell, which was confirmed by the Analyst

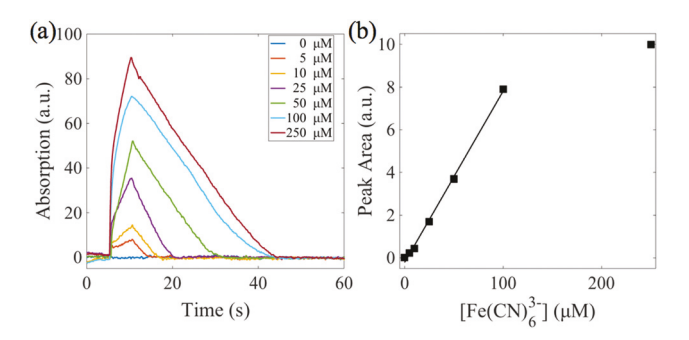


Fig. 3 (a) Absorbance of MV in the reporter cell in repsonse to a potential pulse (3 v, 5 s) applied to the analytical cell at different $Fe(CN)_6^{3-}$ concentrations. (b) Peak area of absorption wave as a function of $Fe(CN)_6^{3-}$ concentration and a linear fit for data below 100 μm .

CCD data, as shown in the 0 µM curve, Fig. 3(a). Thus, no redox reaction occurs to drive color change in the absence of the analyte, $\mathrm{Fe}(\mathrm{CN})_6{}^{3-}$. In contrast, when the analytical cell is filled with Fe(CN)₆³⁻, absorption resulting from the reduction of MV²⁺ to MV⁺⁺ increases monotonically during the 5 s period of the applied potential pulse and returns to baseline level when the potential is removed. Fig. 3 clearly indicates that the magnitude of the absorption varies with analyte concentration and is linear at concentrations below 100 µM. The saturation of the signal above 100 µM likely results from saturation of the absorption, not non-linearity in the electrochemistry at WE_a. Another possible factor is that the amount of MV*+ produced is no longer proportional to the concentration of $Fe(CN)_6^{3-}$, since the redox event depends on the redox reactions at both cells and their coupling efficiency.²⁸ By comparing the sensitivity obtained from Fig. 3(b) to fluctuations in the control experiment, 0 µM, Fig. 3(a), a limit of detection (LOD) of 1.0 µM was obtained.

Smartphone detection and RGB analysis

In the previous section, the color change in the reporter cell induced by reaction of analyte in the analytical cell was demonstrated by measuring the change in absorption in the reporter cell, as measured by a CCD camera. In order to move the device toward a field-deployable format, the CCD camera was replaced by smartphone-based detection. Images of the reporter cell at different analyte concentrations were acquired by a smartphone camera, and RGB analysis was performed on the resulting color images. Fig. 4(a) shows the images of the MV*+ as Fe(CN)₆ 3- was tested at different concentrations. It can readily be seen that the color of the images changes in the presence of Fe(CN)₆³⁻, becoming darker at higher concentrations. The lowest concentration of $Fe(CN)_6^{3-}$ in the analytical cell that could drive color change detectable by naked eye in the reporter cell was ${\sim}10~\mu M$. When the $Fe(CN)_6^{3-}$ exceeds 100 µM, the difference of color change due to the increase of Fe(CN)₆³⁻ concentration becomes indistinguishable visually. These results are consistent with the above observations obtained with a CCD camera.

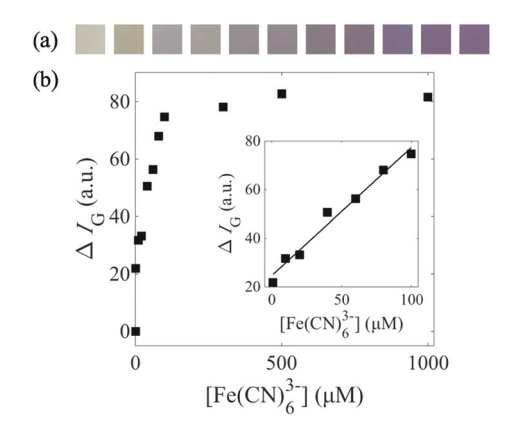


Fig. 4 (a) Images of the MV solution in the reporter cell taken by smartphone at different concentrations of Fe(CN)₆³⁻ in the analytical cell, increasing from 0 µm (left) to 1 mm (right). (b) Change in the green channel signal intensity (δi_{q}) from rgb analysis of images in panel (a), and a linear fit of the data for concentrations below 100 μm (inset).

RGB analysis of the smartphone-acquired images is shown in Fig. 4(b), where signals from green channel were used, because the green channel exhibited somewhat better sensitivity than the red and blue channels. Consistent with the data acquired by CCD camera in Fig. 3, the data plotted in Fig. 4 demonstrate a linear response for $Fe(CN)_6^{3-}$ between 10 to 100 µM. These results confirm the applicability of the smartphone for BPE colorimetric detection of the electrochromic indicator, MV2+, with similar sensitivity as an electron-multiplier CCD camera coupled to a low-power optical microscope. The consilience of the CCD and smartphone camera results is important for field applications, as the cost of the smartphone is ca. 100× less than that of the CCD camera, and the smartphone is, of course, field-portable.

To illustrate the breadth of possible applications, the BPEenabled electrochromic detection scheme was then used for the analysis of a neurotransmitter, dopamine (DA), and a pain medication, acetaminophen (AP). Fig. 5 shows the results of an RGB analysis of the images taken by a smartphone for both DA and AP. Similar to the results obtained for $Fe(CN)_6^{3-}$, increasing analyte concentrations in the analytical cell lead to

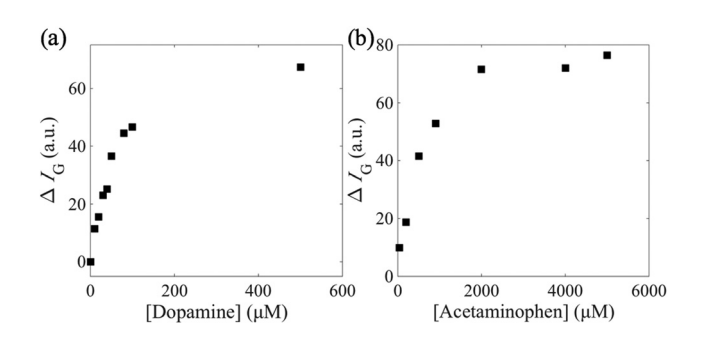


Fig. 5 Change in the green channel signal intensity (δi_q) as a function of dopamine, (a), and acetaminophen, (b), concentration in a BPE-enabled electrochromic sensor using a smartphone and RGB analysis.

Paper Analyst

larger MV*+ concentration and stronger absorption, exhibiting a linear region at low concentration and then a saturated region at high concentration of analyte. In the case of DA, the linear dynamic range is similar to that of $Fe(CN)_6^{3-}$, ranging to ca. 100 µM. On the other hand, RGB analysis of the smartphone images acquired from the reporter cell with increasing AP concentration in the analytical cell, Fig. 5(b), shows a linear range changes to ~500 µM, and saturated signal above [AP] ~2 mM. The likely reason for this observation is that the acetaminophen undergoes a quasireversible reaction⁵⁵ at the WE and is the factor limiting the coupling efficiency in the BPE-enabled device. This is an intrinsic feature of BPEcoupled reactions in the closed BPE configuration, specifically because redox reactions of acetaminophen in the analytical cell are limited by the need for the BPE electrode to have access to a reversible reaction to balance the change of the charge in the chamber. Nevertheless, these results confirm that the BPE-coupled electrochromic effect can be extended beyond model analytes and applied to the determination of organic analytes of biomedical interest. In addition, the BPE detector presented here is compatible with a diverse set of electrochemical sensing techniques, such as those used for monitoring of glucose, cholesterol, and other health-related analytes. The physical separation of the analytical and reporter compartments serves to minimize the interference of the reporter system with the enzyme immobilized on the sensing electrode. The simple configuration and low cost of the device also suggests applications in the environmental monitoring, especially in resource-limited settings.

Battery-based electrochromic sensor

The results described in the previous section were obtained from a closed BPE-enabled device with applied potentials controlled by a potentiostat. Using batteries to replace a potentiostat represents an opportunity to further simplify the sensing scheme and, together with smartphone image acquisition, realize a portable, low cost device for electrochemical detection. In this experiment, two AA batteries in series were used to provide a steady output voltage of ~3.0 V, which is similar to the potential applied by the potentiostat in the previous experiments. Fig. 6(a) shows the optical images captured by a smartphone camera, and Fig. 6(b) shows the green channel RGB results for measurements of Fe(CN)₆³⁻ at varying concentration. Similar to the results described above, in which a potentiostat was used (Fig. 4), the color of the images changes from colorless to increasingly deeper purple with increasing $Fe(CN)_6^{3-}$ concentration. These visual observations are confirmed by the RGB results which display both linear and saturated regions similar to those obtained using a potentiostat for potential control. The linear dynamic range obtained with battery-powered operation is somewhat smaller than that obtained with a potentiostat (Fig. 4), however these experiments do illustrate the possibility of using batteries to drive BPE-enabled colorimetric sensing with µM sensitivity.

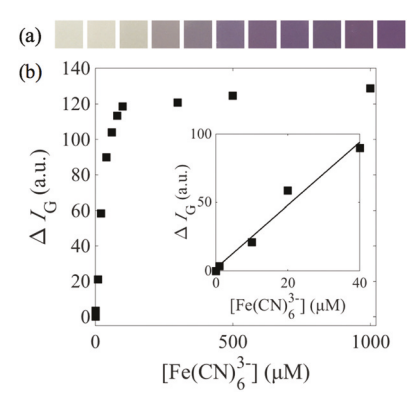


Fig. 6 (a) images of the MV solution in the reporter cell taken by a smartphone in a BPE-enabled electrochromic sensor in which the analytical reaction is driven by batteries. images were acquired at different concentration of $Fe(CN)_6^{3-}$, increasing from 0 μ m (left) to 1 mm (right). (b) change in δi_g from images in panel (a), and a linear fit of the data for concentrations lower than 40 μ m (inset).

BPE-enabled detection in non-aqueous systems

The use of a closed-BPE system allows the analyte and reporter cells to have distinct properties and even chemical compositions. In order to evaluate the applicability of the BPEenabled electrochromic sensor for measurements in nonaqueous solutions, ferrocene (Fc) in acetonitrile was used as the analyte, and it was coupled to the aqueous MV²⁺ reporter system in a closed-BPE configuration. Fig. 7 shows an example of the MV²⁺ color change upon reaction of Fc in 0.1 M TBATPB in acetonitrile. Compared with control experiments with supporting electrolyte alone, a color change can be detected visually down to 1 µM Fc. Increasing the Fc to 100 µM, a darker color was observed. This result was also confirmed by CCD camera measurements, consistent with the results obtained using Fe(CN)₆³⁻ in aqueous solution (Fig. 3). It is interesting to note that Fc in acetonitrile is more effective in driving the BPE reactions than $Fe(CN)_6^{3-}$. Visual detection of

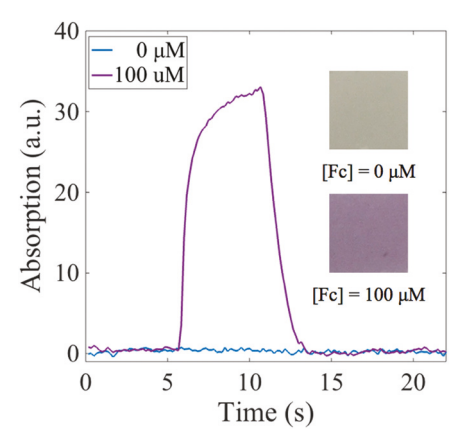


Fig. 7 Absorption of MV in the reporter cell changing as a function of concentration of Fc in the analytical cell upon applying a potential pulse (2 v, 5 s), and the corresponding images captured by a smartphone (inset).

the MV^{2+} color change could be achieved for Fc concentrations as low as 1 μ M Fc compared to 10 μ M Fe(CN)₆³⁻. This could be the result of the ideal redox reversibility of Fc and its large diffusion coefficient (2.5 × 10⁻⁹ m² s⁻¹) in acetonitrile, both of which contribute to higher coupling efficiency for redox reactions at the closed-BPE. By comparing the sensitivity for Fc detection to fluctuations in a control experiment, *e.g.* blue line in Fig. 7, an LOD of 0.3 μ M for Fc detection was obtained.

Conclusions

A closed-BPE-enabled colorimetric device has been developed for electrochemical sensing in both aqueous and non-aqueous systems by exploiting the electrochromic behavior of methyl viologen as a reporter. In the device, electrochemical reactions occurring in the analytical cell are coupled to electrochromic reduction of colorless MV²⁺ to purple MV⁺⁺ in the reporter cell, resulting in a color change that can be captured by electron-multiplied CCD camera, smartphone camera, or even visually. Furthermore, the applied potentials can be controlled either conventionally with a potentiostat, or with simple AA batteries. The combination of battery-powered operation of a compact closed-BPE dual cell configuration with resulting color changes being captured with a smartphone camera yields a simple, inexpensive, field-deployable electrochemical sensor.

In order to characterize the analytical figures of merit, Fe(CN)₆³⁻ and Fc were used as analytes, and the MV²⁺ color change was measured, demonstrating a strong dependence MV²⁺ absorption change on analyte concentration. A linear dynamic range from 10 µM to 100 µM and an LOD of 1.0 µM were achieved for Fe(CN)₆³⁻ in aqueous solution, while an LOD of 0.3 µM was determined for Fc in acetonitrile. The analytical figures of merit are almost certainly influenced strongly by the cell design, since the electrode spacing plays a major role in the limiting transport processes that couple reactions at the WEa and BPEa in the analytical cell and the BPEr and CE/QRE in the reporter cell. In the experiments reported here the goal was to achieve a simple device architecture that could support field-deployable applications, rather than to optimize analytical performance. One could alternatively, improve performance by decreasing the WE-BPE distance (50 µm in these experiments) and by increasing the geometric efficiency of the electrodes, for example by using interdigitated electrode arrays. Altogether, the demonstrated operating features make the BPE-enabled colorimetric device a promising platform for a variety of electrochemical sensing applications where low cost and simple operation are key attributes.

Acknowledgements

This work was supported by the Department of Energy Office of Basic Energy Sciences through grant DE FG02 07ER15851 (WX) and by the National Science Foundation grant

NSF1404744 (KF & CM). This manuscript is dedicated to the memory of our late friend and colleague Craig Lunte.

References

- 1 S. E. Fosdick, K. N. Knust, K. Scida and R. M. Crooks, *Angew. Chem., Int. Ed.*, 2013, 52, 10438–10456.
- 2 G. Loget, D. Zigah, L. Bouffier, N. Sojic and A. Kuhn, Acc. Chem. Res., 2013, 46, 2513–2523.
- 3 F. Mavre, R. K. Anand, D. R. Laws, K. F. Chow, B. Y. Chang, J. A. Crooks and R. M. Crooks, *Anal. Chem.*, 2010, 82, 8766– 8774.
- 4 G. Loget and A. Kuhn, *Anal. Bioanal. Chem.*, 2011, 400, 1691–1704.
- 5 J. C. Bradley, H. M. Chen, J. Crawford, J. Eckert, K. Ernazarova, T. Kurzeja, M. D. Lin, M. McGee, W. Nadler and S. G. Stephens, *Nature*, 1997, 389, 268–271.
- 6 C. Warakulwit, T. Nguyen, J. Majimel, M. H. Delville, V. Lapeyre, P. Garrigue, V. Ravaine, J. Limtrakul and A. Kuhn, *Nano Lett.*, 2008, 8, 500–504.
- 7 C. Ulrich, O. Andersson, L. Nyholm and F. Bjorefors, *Angew. Chem., Int. Ed.*, 2008, 47, 3034–3036.
- 8 S. Ramakrishnan and C. Shannon, *Langmuir*, 2010, 26, 4602–4606.
- 9 R. Ramaswamy and C. Shannon, *Langmuir*, 2011, 27, 878–881.
- 10 N. Shida, F. Kitamura, T. Fuchigami, I. Tomita and S. Inagi, ChemElectrochem, 2016, 3, 465–471.
- 11 W. Zhan, J. Alvarez and R. M. Crooks, *J. Am. Chem. Soc.*, 2002, **124**, 13265–13270.
- 12 B. Y. Chang, K. F. Chow, J. A. Crooks, F. Mavre and R. M. Crooks, *Analyst*, 2012, 137, 2827–2833.
- 13 X. W. Zhang, C. G. Chen, J. Li, L. B. Zhang and E. K. Wang, *Anal. Chem.*, 2013, **85**, 5335–5339.
- 14 S. E. Fosdick, S. P. Berglund, C. B. Mullins and R. M. Crooks, *Anal. Chem.*, 2013, **85**, 2493–2499.
- 15 S. E. Fosdick and R. M. Crooks, J. Am. Chem. Soc., 2012, 134, 863–866.
- 16 S. E. Fosdick, S. P. Berglund, C. B. Mullins and R. M. Crooks, ACS Catal., 2014, 4, 1332–1339.
- 17 J. Wang and K. M. Manesh, Small, 2010, 6, 338-345.
- 18 Y. Wang, R. M. Hernandez, D. J. Bartlett, J. M. Bingham, T. R. Kline, A. Sen and T. E. Mallouk, *Langmuir*, 2006, 22, 10451–10456.
- 19 G. Loget and A. Kuhn, J. Am. Chem. Soc., 2010, 132, 15918– 15919.
- 20 D. Hlushkou, R. K. Perdue, R. Dhopeshwarkar, R. M. Crooks and U. Tallarek, *Lab Chip*, 2009, 9, 1903– 1913.
- 21 D. R. Laws, D. Hlushkou, R. K. Perdue, U. Tallarek and R. M. Crooks, *Anal. Chem.*, 2009, **81**, 8923–8929.
- 22 E. Sheridan, D. Hlushkou, K. N. Knust, U. Tallarek and R. M. Crooks, *Anal. Chem.*, 2012, **84**, 7393–7399.
- 23 R. K. Perdue, D. R. Laws, D. Hlushkou, U. Tallarek and R. M. Crooks, *Anal. Chem.*, 2009, **81**, 10149–10155.

- 24 B. Y. Chang, J. A. Crooks, K. F. Chow, F. Mavre and R. M. Crooks, J. Am. Chem. Soc., 2010, 132, 15404-
- 25 R. Dhopeshwarkar, D. Hlushkou, M. Nguyen, U. Tallarek and R. M. Crooks, J. Am. Chem. Soc., 2008, 130, 10480-10481.
- 26 K. F. Chow, F. Mavre and R. M. Crooks, J. Am. Chem. Soc., 2008, 130, 7544-7545.
- 27 J. T. Cox, J. P. Guerrette and B. Zhang, Anal. Chem., 2012, 84, 8797-8804.
- 28 J. P. Guerrette, S. M. Oja and B. Zhang, Anal. Chem., 2012, 84, 1609-1616.
- 29 X. W. Zhang, J. Li, X. F. Jia, D. Y. Li and E. K. Wang, Anal. Chem., 2014, 86, 5595-5599.
- 30 X. W. Zhang, C. G. Chen, J. Y. Yin, Y. C. Han, J. Li and E. K. Wang, Anal. Chem., 2015, 87, 4612-4616.
- 31 M. S. Wu, Z. Liu, J. J. Xu and H. Y. Chen, ChemElectrochem, 2016, 3, 429-435.
- 32 S. Z. Wu, Z. Y. Zhou, L. R. Xu, B. Su and O. Fang, Biosens. Bioelectron., 2014, 53, 148-153.
- 33 M. S. Wu, D. J. Yuan, J. J. Xu and H. Y. Chen, Chem. Sci., 2013, 4, 1182-1188.
- 34 S. M. Oja, J. P. Guerrette, M. R. David and B. Zhang, Anal. Chem., 2014, 86, 6040-6048.
- 35 J. P. Guerrette, S. J. Percival and B. Zhang, J. Am. Chem. Soc., 2013, 135, 855-861.
- 36 C. X. Ma, L. P. Zaino and P. W. Bohn, Chem. Sci., 2015, 6, 3173-3179.
- 37 L. Bouffier, T. Doneux, B. Goudeau and A. Kuhn, Anal. Chem., 2014, 86, 3708-3711.
- 38 W. Xu, C. X. Ma and P. W. Bohn, ChemElectrochem, 2016, 3, 422-428.
- 39 R. Cao, B. X. Li, Y. F. Zhang and Z. N. Zhang, Chem. Commun., 2011, 47, 12301-12303.

- 40 J. F. Zhang, Y. Zhou, J. Yoon and J. S. Kim, Chem. Soc. Rev., 2011, 40, 3416-3429.
- 41 X. H. Cheng, Q. Q. Li, C. G. Li, J. G. Qin and Z. Li, Chem. -Eur. J., 2011, 17, 7276-7281.
- 42 X. H. Cheng, Y. Zhou, J. G. Qin and Z. Li, ACS Appl. Mater. Interfaces, 2012, 4, 2133-2138.
- 43 J. J. Du, L. Jiang, Q. Shao, X. G. Liu, R. S. Marks, J. Ma and X. D. Chen, Small, 2013, 9, 1467-1481.
- 44 R. J. Mortimer, Annu. Rev. Mater. Res., 2011, 41, 241-268.
- 45 D. R. Rosseinsky and R. J. Mortimer, Adv. Mater., 2001, 13, 783-793.
- 46 R. J. Mortimer and T. S. Varley, ol. Energy Mater. Sol. Cells, 2012, 99, 213-220.
- 47 M. Gonsalves, J. V. Macpherson, D. O'Hare, C. P. Winlove and P. R. Unwin, Biochim. Biophys. Acta, 2000, 1524, 66-74.
- 48 L. Shen, J. A. Hagen and I. Papautsky, Lab Chip, 2012, 12, 4240-4243.
- 49 N. Lopez-Ruiz, V. F. Curto, M. M. Erenas, F. Benito-Lopez, D. Diamond, A. J. Palma and L. F. Capitan-Vallvey, Anal. Chem., 2014, 86, 9554-9562.
- 50 Y. Jung, J. Kim, O. Awofeso, H. Kim, F. Regnier and E. Bae, Appl. Opt., 2015, 54, 9183-9189.
- 51 S. K. Vashist, T. van Oordt, E. M. Schneider, R. Zengerle, F. von Stetten and J. H. T. Luong, Biosens. Bioelectron., 2015, 67, 248-255.
- 52 H. J. Nie, W. Wang, W. Li, Z. Nie and S. Z. Yao, Analyst, 2015, 140, 2771-2777.
- 53 C. X. Ma, N. M. Contento, L. R. Gibson and P. W. Bohn, ACS Nano, 2013, 7, 5483-5490.
- 54 M. A. G. Zevenbergen, B. L. Wolfrum, E. D. Goluch, P. S. Singh and S. G. Lemay, J. Am. Chem. Soc., 2009, 131, 11471-11477.
- 55 N. Wangfuengkanagul and O. Chailapakul, J. Pharmaceut. Biomed., 2002, 28, 841-847.